Wu *et al.*
Chinese Journal of Mechanical Engineering (2023) 36:4
https://doi.org/10.1186/s10033-022-00825-x

Chinese Journal of Mechanical Engineering

ORIGINAL ARTICLE **Open Access**

Experimental Research on the Surface Quality of Milling Contour Bevel Gears

Mingyang Wu[1,2*], Jianyu Zhang[1,2], Chunjie Ma[1,2], Yali Zhang[1,2] and Yaonan Cheng[1,2]

Abstract

Contour bevel gears have the advantages of high coincidence, low noise and large bearing capacity, which are widely used in automobile manufacturing, shipbuilding and construction machinery. However, when the surface quality is poor, the effective contact area between the gear mating surfaces decreases, affecting the stability of the fit and thus the transmission accuracy, so it is of great significance to optimize the surface quality of the contour bevel gear. This paper firstly analyzes the formation process of machined surface roughness of contour bevel gears on the basis of generating machining method, and dry milling experiments of contour bevel gears are conducted to analyze the effects of cutting speed and feed rate on the machined surface roughness and surface topography of the workpiece. Then, the surface defects on the machined surface of the workpiece are studied by SEM, and the causes of the surface defects are analyzed by EDS. After that, XRD is used to compare the microscopic grains of the machined surface and the substrate material for diffraction peak analysis, and the effect of cutting parameters on the microhardness of the workpiece machined surface is investigated by work hardening experiment. The research results are of great significance for improving the machining accuracy of contour bevel gears, reducing friction losses and improving transmission efficiency.

Keywords Contour bevel gear, Machined surface quality, Surface roughness, Surface defect, Surface morphology

1 Introduction

Contour bevel gears are the essential components for the transmission of motion between intersecting and staggered axes with the advantages of good meshing performance, smooth transmission, high bearing capacity, low noise, etc. They are widely used in automotive, engineering machinery, aerospace, mining, metallurgy, petroleum and other industrial fields. The quality of the machined surface has a significant effect on the matching accuracy, wear resistance, fatigue resistance, corrosion resistance and transmission performance of contour bevel gears. The manufacturing accuracy of contour bevel gears directly affects the transmission efficiency, noise, motion accuracy and service life of the machine. Its true tooth surface morphology is complex, such as machine tool rigidity, cutterhead installation errors and cutting parameters. It restricts the machining accuracy of contour bevel gears seriously. Therefore, it is of great practical significance to study the surface quality of contour bevel gears.

Scholars around the world have conducted different degrees of research on the quality of machined surfaces. Han et al. [1] proposed a central composite surface design method based on response surface methodology and established a regression model for the surface roughness of honing workpiece gears. Khalilpourazary et al. [2] studied the surface roughness of the processed spur gears and found that the arithmetic surface roughness value of the spur gears manufactured with a lubricant containing alumina nanoparticles during the hobbing process was decreased. Ming et al. [3] established an equation for the residual height to improve the surface quality of the face

---

*Correspondence:
Mingyang Wu
13936161878@139.com
[1] School of Mechanical and Power Engineering, Harbin University of Science and Technology, Harbin 150080, China
[2] The Key Laboratory of National and Local United Engineering for "High-Efficiency Cutting and Tools", Harbin 150080, China

gear and modified the grinding surface roughness model of the face gear. Pathak et al. [4] used the surface finish, microstructure, and microhardness to evaluate the surface quality of bevel gears, and they found that honing gears can improve the surface quality of gears and reduce the transmission noise of the machine. Michalski et al. [5] found that the roughness height and roughness spacing were smaller for the tooth point surface than for the root surface after hobbing. Klocke et al. [6] performed a metallographic test on surface defects of gear hobbing, they investigated the effect of the tool and process design on dry hobbing surface defects by comparing the appearance of surface defects and characteristic values generated by the gear hobbing. Han et al. [7] quantitatively analyzed the three-dimensional morphological data of tooth surfaces for two gear finishing processes, grinding and honing, and found that the grinding process could obtain smaller roughness and higher geometric accuracy compared to the honing process, but the residual stresses of the honing process were smaller than those of the grinding process. Zheng et al. [8] proposed an algorithm, which takes the insert run-out errors into consideration, for the roughness of the face-milling spiral bevel gear. Simon [9] proposed a new hobbing model that determines the deviation between machined and theoretical tooth surfaces of spur and helical gears, which can be used to improve the microscopic surface morphology of spur and helical gears. Hassanpour et al. [10] conducted milling tests on 4340 alloy steel, they used response surface methodology to investigate the influences of different cutting parameters on surface roughness, morphology, microhardness, white layer thickness, and surface chemical composition. Mao et al. [11] proposed a tooth grinding method by variable velocity generation machining of variable speed of conical wheels, and it can reduce surface roughness and shorten grinding time remarkably by comparing with the uniform generation machining method. Lin et al. [12] used the roughness profilometer to obtain the measurement data of the tooth profile and formulated the theoretical geometric model of the involute cylindrical gear tooth profile based on the parameters of the tested gear. Bin et al. [13] established a mathematical model for grinding disk wheels based on the principle of CNC grinding by the generating machining method for face gears, considering the influence of grinding wheel morphology and contact deformation during the grinding process. Ma et al. [14] carried out theoretical analysis and experimental research on the surface roughness of the hard tooth surface gear after shaving. They found that the surface roughness of the gear is smaller than that of the general hobs, and decreases with the increase of the negative rake angle of hobs. Gao et al. [15] conducted gear hobbing experiments by selecting different hobs, top edge fillet radius, and hob edge shapes for hobbing experiments. They analyzed the influence of different factors on tooth surface roughness. Li et al. [16] obtained the results of effectively reducing the tooth surface error by automatic identification of tooth surface error and feedback correction of machine tool motion parameters. Wang et al. [17] discretized the tooth surface and gave the radial and normal vectors of the discrete points of the tooth surface according to the mathematical model of the curved bevel gear, and established the expression of the tooth shape error of the modified tooth surface at the discrete points concerning the theoretical tooth surface.

In summary, scholars around the world have conducted research on the machined surface quality of external cylindrical, flat, and standard cylindrical gears and other parts. There are few studies on the machined surface quality of contour bevel gears. Therefore, this paper takes the contour bevel gear as the research object, analyzes the forming process of the machined surface roughness of the workpiece by the generation machining principle of the contour bevel gear. The dry milling experiment of contour bevel gears is carried out, dry milling experiment of contour bevel gears is conducted to study the effect of cutting speed and feed rate on the surface quality of machined surface roughness and surface morphology by single factor method, and to analyze the surface defects of the machined surface by EDS; XRD is used to compare the diffraction peaks of the microscopic grains of the machined surface and the substrate material, and the effect of cutting parameters on the microhardness of the machined surface is studied through work hardening experiment. The above research results not only provide a basis for the optimization of the surface quality and process parameters of contour bevel gears but also have a certain reference value for the research on the machining accuracy and transmission efficiency of contour bevel gears.

2 The Forming Process of Surface Roughness of Milling Contour Bevel Gears

2.1 Generation Machining Principle of Contour Bevel Gears

Generating machining method is usually used for the machining of contour bevel gears, which is based on the rolling engagement between the flat-imaginary gear and the gear blank. The cutting surface of the tool

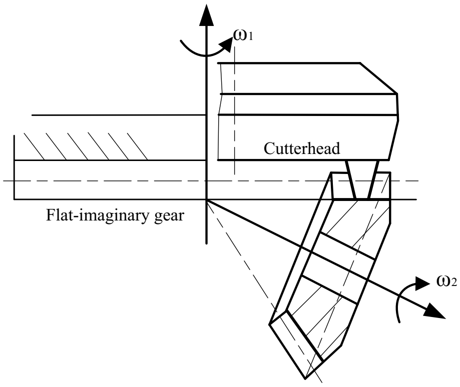

Figure 1 Diagram of the generating machining method for contour bevel gears

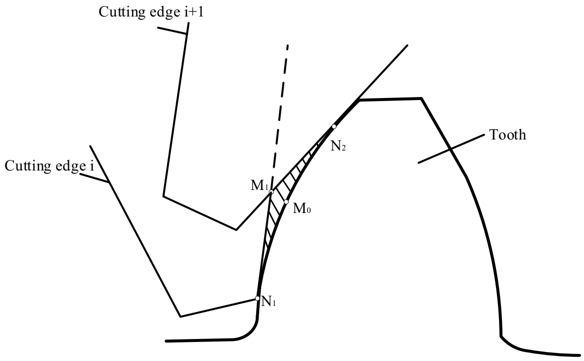

Figure 2 Diagram of roughness formation on machined surfaces

representing the flat-imaginary gear is enveloped around the tooth surface of the gear blank, as shown in Figure 1. In the process of generation machining, the workpiece rotates around its axis, and the cutterhead rotates around the axis of the cradle. Since the machining principles of contour bevel gear and contour bevel pinion are the same, this paper focuses on the generating machining method for machining contour bevel gears.

2.2 The Forming Process of the Residual Height of Milling Contour Bevel Gears

In the actual machining process, without considering the conditions such as tool wear and machine tool vibration, there is only the cutting edge of the blade that participates in the machining. The cutting edges of the cutterhead are discretely distributed. The discrete cutting edges cut the gear blank intermittently with the rotation of the cutterhead, which causes the discontinuity of cutting motion, resulting in cutter marks on the tooth surface after cutting and the existence of residual area.

For generating machining, discontinuous cutting of the cutting edge is one of the main causes of the residual height produced, as shown in Figure 2. The area of the surface M_1-N_1-M_0-N_2 enclosed by the cutting edge i and the cutting edge $(i+1)$ is the residual area, and The line between M_1 and the point M_0 projected to the tooth surface is the residual height.

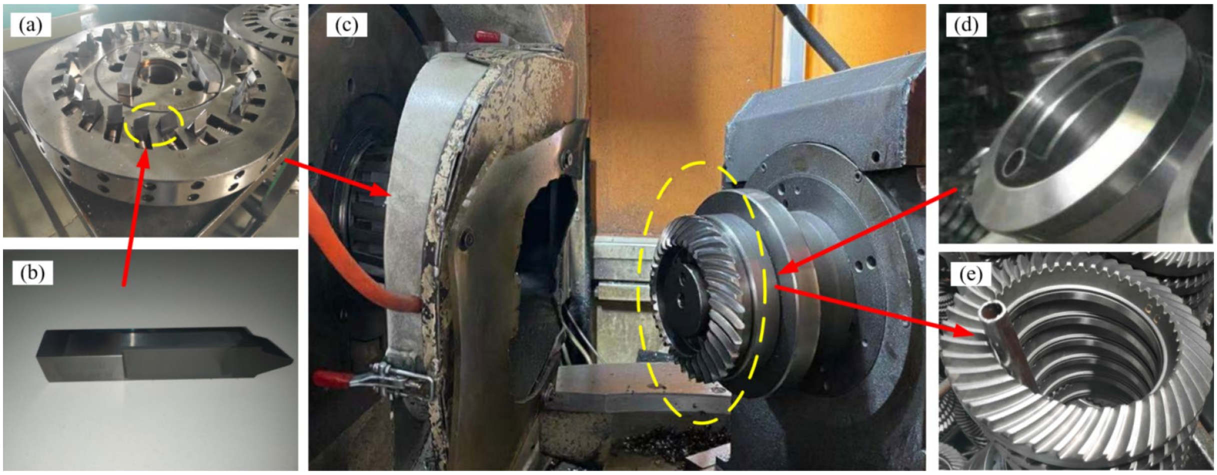

Figure 3 Dry milling machine device for contour bevel gears

Table 1 Chemical composition of 20CrMnTi

Element	C	Si	Mn	Cr	S	P	Ni	Ti
Content	0.18	0.28	0.93	1.12	0.007	0.01	0.0045	0.065

Table 2 Performance parameters of 20CrMnTi material

Density (kg/m^3)	Elastic modulus (GPa)	Thermal expansion coefficient (1/℃)	Poisson's ratio	Hardness (HB)
7800	207	5×10^{-6}	0.25	≤217

Table 3 Cutting parameters

Cutting parameter	Cutting speed *v* (m/min)	Feed rate *f* (mm/r)
1	260	0.1, 0.2, 0.3
2	170, 200, 230	0.1

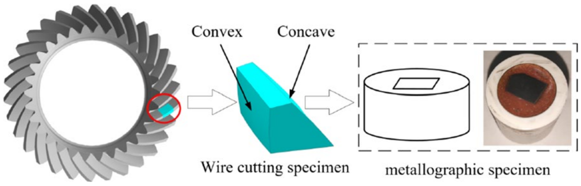

Figure 4 Schematic diagram of metallographic specimen production

3 Milling Experiment of Contour Bevel Gears

3.1 Experiment Conditions and Materials

(1) The CNC machine tool is a Gleason 175HC dry CNC gear milling machine tool. And the specific machining device is shown in Figure 3.

Figure 3(a) shows the cutterhead for machining contour bevel gears, and Figure 3(b) shows the blades, which are divided into internal and external blades. The blades are loaded into the corresponding positions one by one through the tool loader, the screws are tightened to complete the tool loading, and then the assembled cutterhead is loaded onto the tool spindle. Figure 3(d) shows the gear blank of a contour bevel gear, which is clamped in the workpiece spindle of the machine tool by a fixture for machining the contour bevel gear, as shown in Figure 3(c), and Figure 3(e) shows a contour bevel gear after machining.

(2) The workpiece material is 20CrMnTi, the chemical composition and physical properties are shown in Tables 1 and 2.

The experiment tool is formed by the assembly of a Tri-ac cutterhead and DT-270D3-39/8-PN blades, and is processed by the continuous indexing method. That is, the processing of all tooth surfaces of the gear can be machined in one generating machining.

3.2 Experiment Programme Design

The dry milling experiment of contour bevel gears is carried out on the Gleason175HC machine tool. Since the milling process usually uses a one-time feed mode, the main cutting parameters are cutting speed and feed rate. Therefore, the controlled variable method is used to study the influence of the change in the cutting speed and the feed rate on the surface quality of the 20CrMnTi machined surface, to obtain the internal relationship between the processing parameters and the surface quality. The specific single-factor experiment design is shown in Table 3.

3.3 Preparation of Metallographic Specimens

A total of six gears are machined to correspond to the different cutting conditions of the single factor experiment. After that, metallographic specimens with a length of 10 mm and maximum width and height of 5 mm are extracted by slow wire cutting, with each machined gear providing one specimen on the convex and one on the concave side.

The intercepted specimens are fixed using the thermal mosaic method and passed through water sandpaper with mesh numbers of 200, 360, 500, 800, 1000, 1500 and 2000 in turn, from rough grinding to fine grinding, until the surface of the specimen is sanded smooth. Then, the specimen is mechanically polished by the metallographic specimen polishing machine. Finally, the metallographic specimen is chemically etched, and the etchant is 4% nitric acid alcohol, as shown in Figure 4. The microscopic morphology of metallographic specimens is observed by a digital microscope.

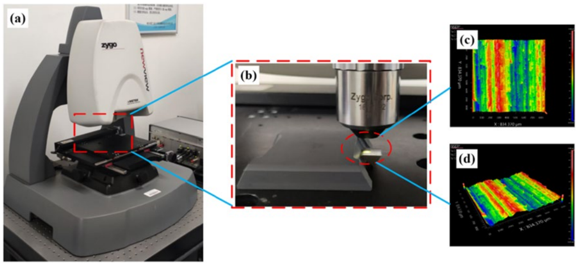

Figure 5 Schematic diagram of the machined surface topography

4 Milling Experiment Results of Contour Bevel Gears

4.1 Surface Roughness Analysis of Milling Contour Bevel Gears

The prepared wire cutting specimens are used to observe the surface morphology by the white light interferometer, Figure 5 is the diagram of the white light interferometer measurement.

Figure 5(a) shows the white light interferometer Zygo New View 8200, the 10× (0.83 mm × 0.83 mm) lens is used to measure wire cutting specimens of the machined surfaces of the contour bevel gears; Figure 5(b) shows the measurement position of the specimen; Figure 5(c) shows the measured two-dimensional surface morphology, and Figure 5(d) shows the three-dimensional surface morphology.

(1) The machined surface morphologies at different feed rates are shown in Figures 6, 7, 8.

The machined surface morphology of contour bevel gears with different feed rates is shown in Figures 6, 7, 8. The colour of surface morphology transitions from blue to red, representing the residual height of the machined surface from low to high. With the increase of feed rate, the distance between the ridge lines on the three-dimensional morphology of the machined surface increases gradually, and the colour difference of the three-dimensional morphology becomes more serious, so the surface roughness increases. The right vertical axis of the roughness distribution curve is the percentage, which represents the relative percentage of the number of three-dimensional points of surface roughness in different regions, and the left vertical axis is count,

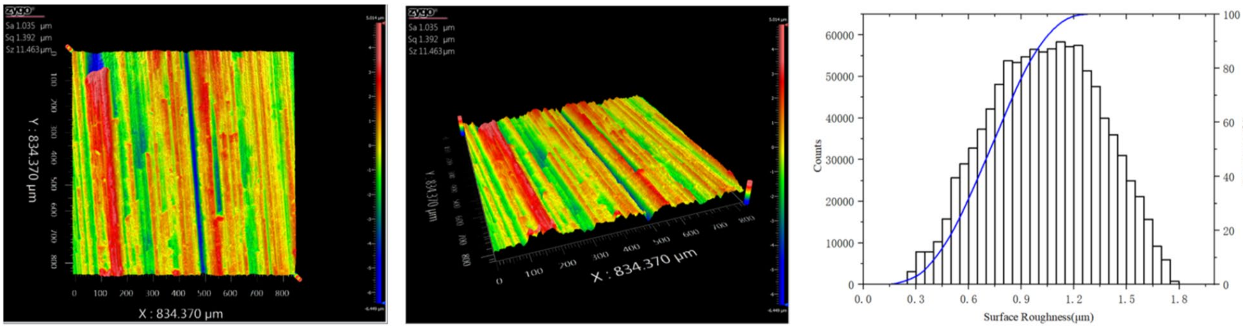

Figure 6 (*f* = 0.1 mm/r, *v* = 260 m/min) 3D morphology, 2D morphology and roughness distribution curve of machined surface

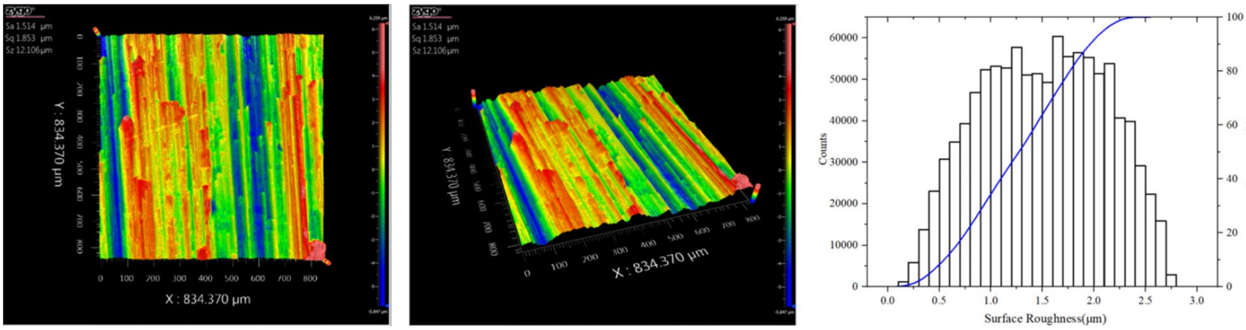

Figure 7 (*f* = 0.2 mm/r, *v* = 260 m/min) 3D morphology, 2D morphology and roughness distribution curve of machined surface

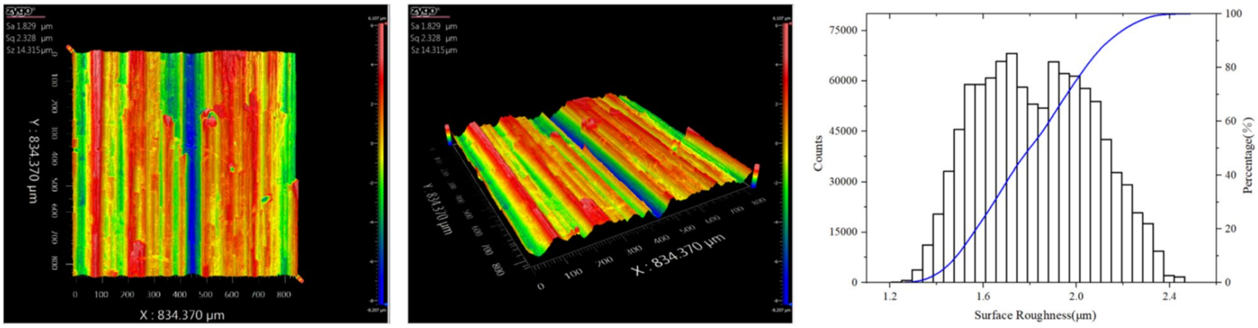

Figure 8 (*f* = 0.3 mm/r, *v* = 260 m/min) 3D morphology, 2D morphology and roughness distribution curve of machined surface

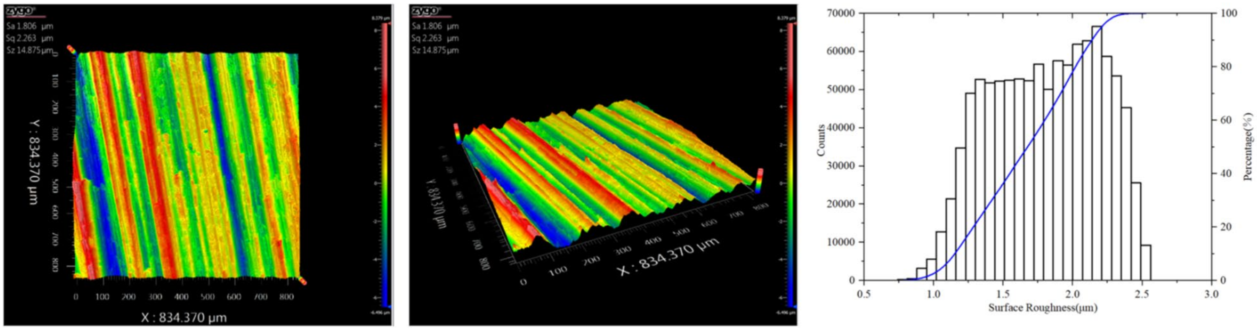

Figure 9 (*f* = 0.1 mm/r, *v* = 170 m/min) 3D morphology, 2D morphology and roughness distribution curve of machined surface

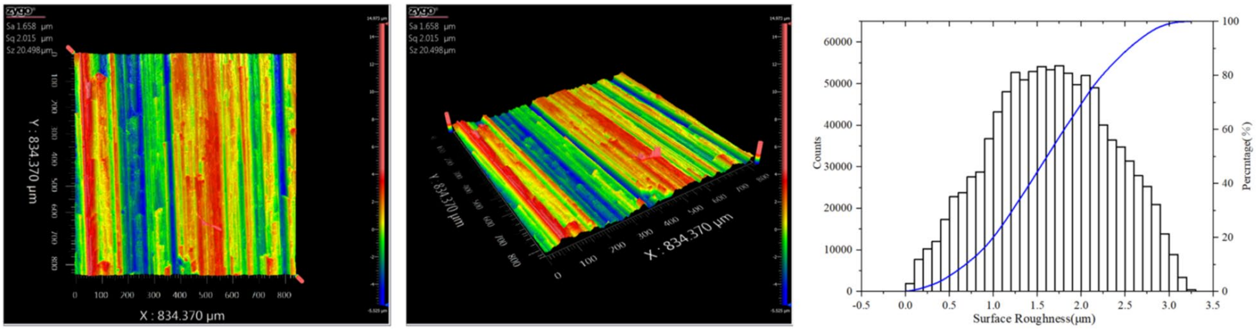

Figure 10 (*f* = 0.1 mm/r, *v* = 200 m/min) 3D morphology, 2D morphology and roughness distribution curve of machined surface

which represents the number of three-dimensional points of surface roughness in different regions. It can be found that, when the feed rate is 0.1 mm/r, the machined surface roughness is concentrated on both sides of the peak, and the surface quality is good.

(2) The machined surface morphologies at different cutting speeds are shown in Figures 9, 10, 11.

The two-dimensional and three-dimensional morphologies of the machined surface of the contour bevel gears obtained at different cutting speeds under dry milling conditions are shown in Figures 9, 10, 11. It can be found that as the cutting speed increases, tool marks of the machined surface gradually become denser, the red part also slowly decreases, and the surface roughness becomes

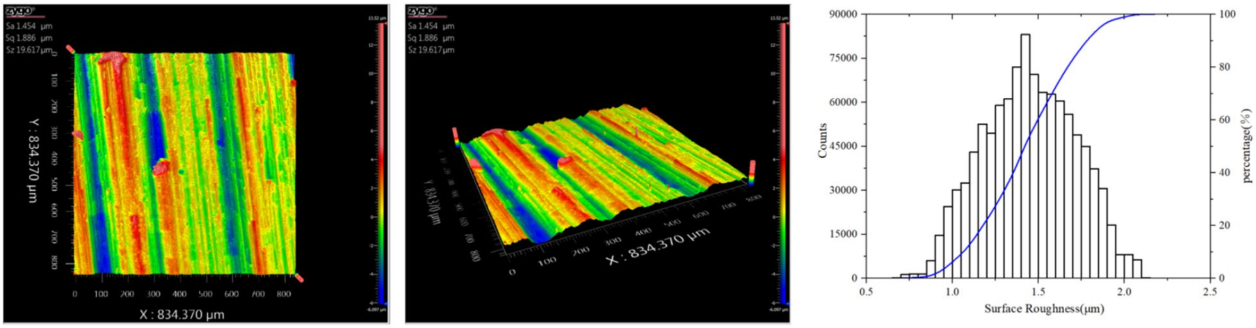

Figure 11 ($f = 0.1$ mm/r, $v = 230$ m/min) 3D morphology, 2D morphology and roughness distribution curve of machined surface

Table 4 Measurement data of machined surface roughness ($f = 0.1$ mm/r)

Cutting parameters	**$v = 170$ m/min**		**$v = 200$ m/min**		**$v = 230$ m/min**	
	Convex	**Concave**	**Convex**	**Concave**	**Convex**	**Concave**
Average deviation of surface arithmetic (S_a)	2.047	1.849	1.673	1.739	1.404	1.437
Surface root mean square deviation (S_q)	2.545	2.250	2.016	2.103	1.766	1.751
Surface ten-point average deviation (S_z)	15.208	13.452	20.993	15.473	14.991	11.944

Table 5 Measurement data of machined surface roughness ($v = 260$ m/min)

Cutting parameters	**$f = 0.1$ mm/r**		**$f = 0.2$ mm/r**		**$f = 0.3$ mm/r**	
	Convex	**Concave**	**Convex**	**Concave**	**Convex**	**Concave**
Average deviation of surface arithmetic(S_a)	1.307	1.222	1.755	1.589	1.967	1.806
Surface root mean square deviation (S_q)	1.589	1.511	2.146	1.985	2.51	2.476
Surface ten-point average deviation (S_z)	10.905	10.787	14.29	13.604	16.933	15.692

smaller. Therefore, within a reasonable range, increasing the cutting speed can optimize the machined surface quality and the machining efficiency. The roughness distribution curve shows that when the cutting speed is 230 m/min, the machined surface roughness is concentrated on both sides of the peak.

The surface roughness of the workpiece machined surface can be obtained by the white light interferometer. To avoid the error caused by a single experiment, the convex and concave surfaces of each tooth surface are measured three times, and the average surface roughness is taken, then the surface roughness at different cutting speeds is shown in Table 4, and the surface roughness at different feed rates is shown in Table 5. The surface arithmetic mean deviation S_a, surface root mean square deviation S_q, and surface ten-point mean deviation S_z can be expressed as [18]

$$S_a = \frac{1}{mn}\sum_{i=1}^{m}\sum_{j=1}^{n}\left|\eta_{ij}\right|, \tag{1}$$

$$S_q = \sqrt{\frac{1}{mn}\sum_{i=1}^{m}\sum_{j=0}^{n}\eta_{ij}^2}, \tag{2}$$

$$S_z = \frac{\sum\limits_{i=1}^{5}\eta_{pi} - \sum\limits_{j=1}^{5}\eta_{vi}}{5}, \tag{3}$$

where, i and j represent the position of row i and column j data of the surface; m is the row number of the measured surface data; n is the column number; η_{pi} and η_{vi} are the first five maximum peaks and the first five deepest valleys of the surface.

It can be seen from Table 4, keeping the feed rate constant and increasing the cutting speed from 170 to

230 m/min, the surface roughness S_a of the convex surface decreases from 2.047 to 1.404 μm, and the surface roughness S_a of the concave surface decreases from 2.047 to 1.404 μm. As shown in Table 5, with the gradual increase of the feed rate, the surface roughness S_a of the convex surface increases from 1.307 to 1.967 μm, the concave of that increased from 1.222 to 1.806 μm, and the change patterns of S_q and S_a are the same, decreasing with the increase of the cutting speed and increasing with the increase of the feed rate.

According to the test results of the machined surface roughness of the contour bevel gears, a prediction model of the machined surface roughness is established as Eq. (4).

$$S_a = Kv^a f^b, \tag{4}$$

where, K is the estimated value of the coefficient, and a and b are respectively the coefficients of the cutting speed v and the feed rate f.

The data in Tables 4 and 5 are respectively put into Eq. (4) to obtain the roughness prediction models of convex and concave surfaces, as shown in Eqs. (5) and (6).

$$S_{a(convex)} = 1\,193.78v^{-1.06}f^{0.41}, \tag{5}$$

$$S_{a(convace)} = 685.31v^{-0.99}f^{0.33}. \tag{6}$$

To verify the accuracy of the established machined surface roughness model, two sets of data in Tables 4 and 5 are selected for testing. The relative error between the experimental and theoretical values can prove the accuracy of the model, and the specific surface roughness error analysis results are shown in Table 6.

From Table 6, it can be found that the average error of several sets of data is 4.16% < 5%, which proves that the roughness prediction model established in this paper can be used for the prediction of the machined surface roughness of the milling contour bevel gears.

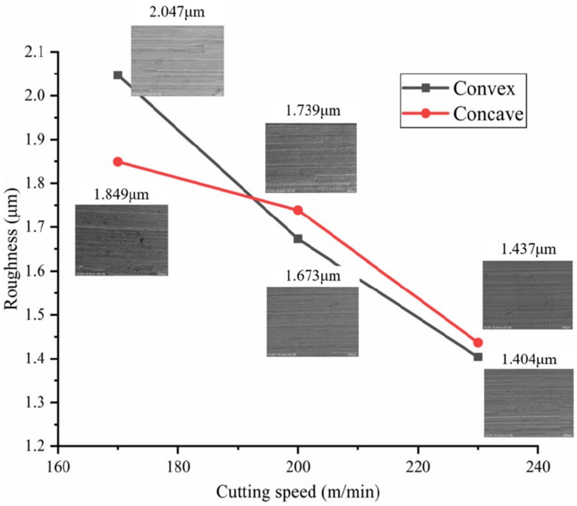

Figure 12 Effect of cutting speed on the morphology of machined concave and convex surfaces

4.2 Surface Morphology Analysis of Milling Contour Bevel Gears

The wire cutting specimens are cleaned by ultrasonic to remove oil and impurities; the influence of cutting parameters on the surface morphology of the concave and convex surfaces of the machined workpiece is analyzed by scanning electron microscopy.

Combined with the machined surface roughness values, the effect of cutting speed on surface morphology is investigated when the feed rate is 0.1 mm/r, as shown in Figure 12. From the roughness graph in Figure 12 and the workpiece surface morphology, it can be found that the increase in cutting speed can reduce the workpiece surface roughness and form a good surface quality. However, due to the influence of cutting heat and tool wear on the surface of the workpiece during the cutting process, the surface roughness difference between the concave and convex surfaces of the gear changes slightly. The roughness of convex is large at the beginning, and smaller than concave as the cutting speed increases. When the cutting speed is 230 m/min, the roughness difference between the convex surface and the concave surface of

Table 6 Analysis results of surface roughness error

Number	Cutting speed v (m/min)	Feed rate f (mm/r)	Convex Surface Roughness (μm)		Relative error (%)	Convace Surface Roughness (μm)		Relative error (%)
			Test value	Predictive value		Test value	Predictive value	
1	200	0.1	1.673	1.737	3.68	1.739	1.673	3.80
2	260	0.2	1.755	1.647	6.15	1.589	1.541	3.02

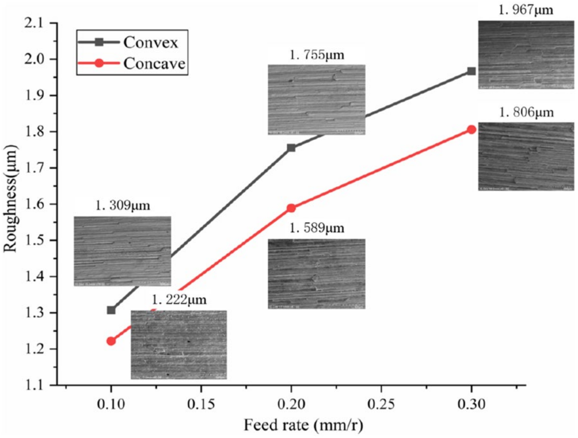

Figure 13 Influence of feed rate on the morphology of machined concave and convex surfaces

the contour bevel gear is the smallest. Therefore, this cutting speed range is more suitable for machining.

Figure 13 shows the influence of the feed rate on the surface morphology at the cutting speed of 260 m/min. It can be found that the machined surface roughness of contour bevel gear gradually increases with the increase of the feed rate, which has a significant impact on the machined surface morphology, resulting in deterioration of the machined surface quality.

4.3 Research on Machined Surface Defects

In the dry milling process of contour bevel gears, surface defects such as tool marks, surface scratch marks, adherent particles, and surface pits will cause impacts on the machined surface quality, so it is necessary to analyze the causes of surface defects by SEM and EDS.

Figure 14(a) and (b) is the microscopic surface morphologies of the contour bevel gear at v = 260 m/min, f = 0.3 mm/r. It can be found that there is surface adhesion on the machined surface of the gear, which is due to the chemical interaction between the surface material with the oxygen element in the air under the high cutting temperature and cutting stress conditions, resulting in oxide adsorption on the machined surface and formation of irregular bulges. Figure 14(c) is a partially enlarged drawing of Figure 14(a), and it can be noticed that the surface defects are unfolded along the direction of the cutter mark. Figure 14(d) shows the microscopic surface morphology of the contour bevel gear at v = 260 m/min, f = 0.2 mm/r; during the gear machining process, part of the cutting chips is adsorbed on the machined surface of the workpiece. The surface adsorption is formed with high cutting stress, which increases the roughness value

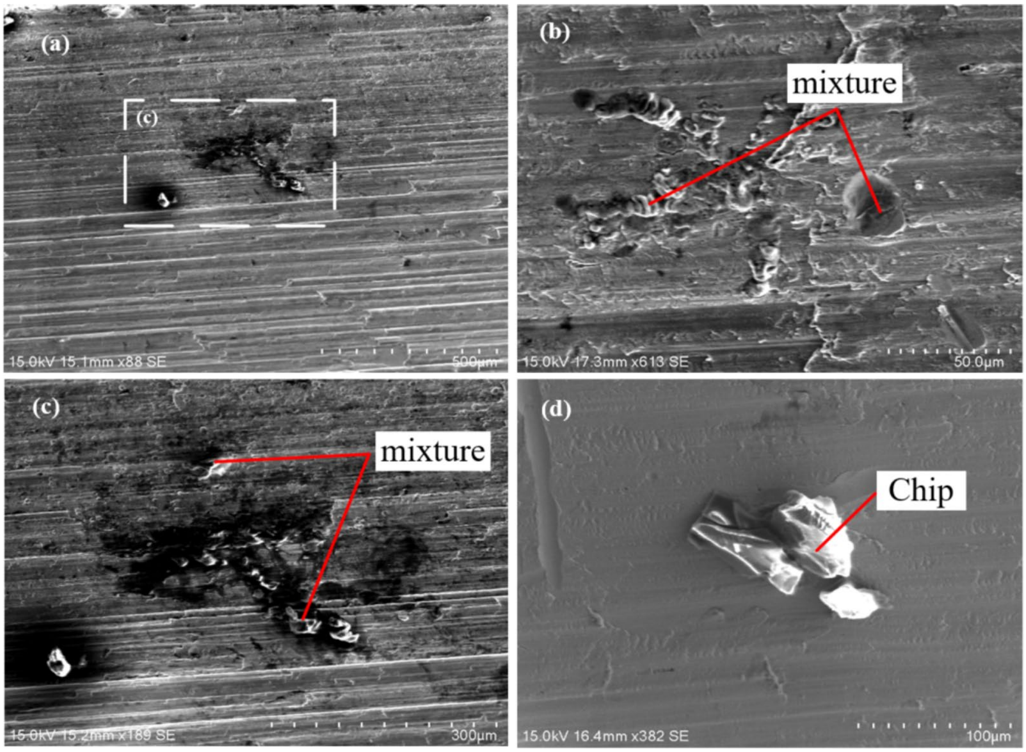

Figure 14 Surface adhesion of contour tooth bevel gear in dry milling

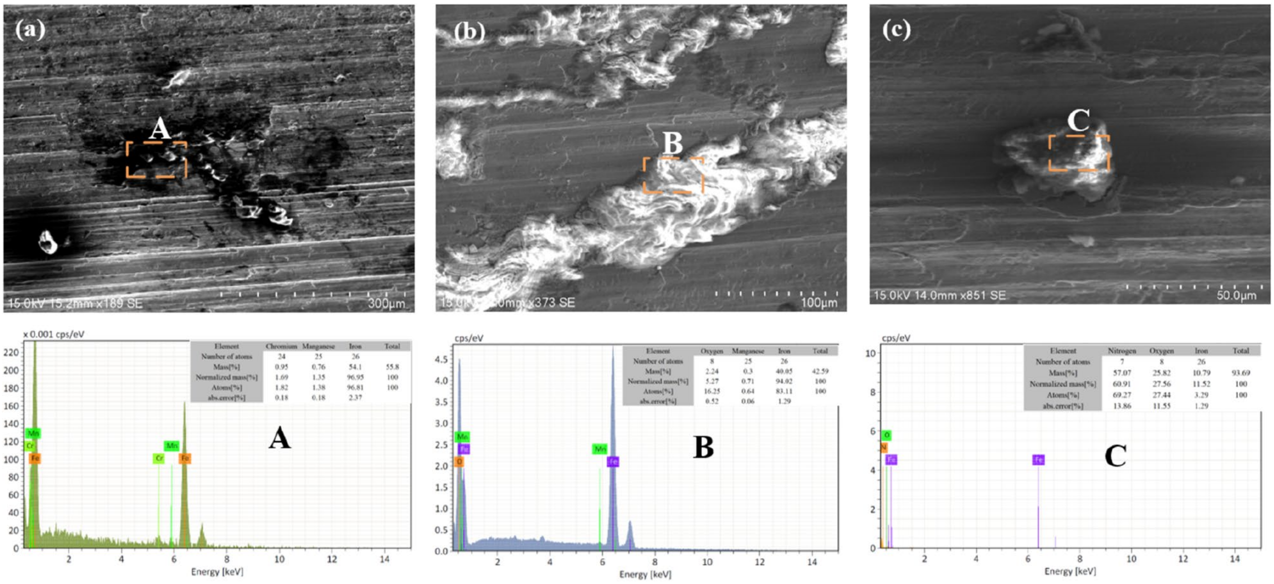

Element	Chromium	Manganese	Iron	Total
Number of atoms	24	25	26	
Mass[%]	0.95	0.76	54.1	55.8
Normalized mass[%]	1.69	1.35	96.95	100
Atoms[%]	1.82	1.38	96.81	100
abs.error[%]	0.18	0.18	2.37	

Element	Oxygen	Manganese	Iron	Total
Number of atoms	8	25	26	
Mass[%]	2.24	0.3	40.05	42.59
Normalized mass[%]	5.27	0.71	94.02	100
Atoms[%]	16.25	0.64	83.11	100
abs.error[%]	0.52	0.06	1.29	

Element	Nitrogen	Oxygen	Iron	Total
Number of atoms	7	8	26	
Mass[%]	57.07	25.82	10.79	93.69
Normalized mass[%]	60.91	27.56	11.52	100
Atoms[%]	69.27	27.44	3.29	100
abs.error[%]	13.86	11.55	1.29	

Figure 15 EDS analysis of surface defects

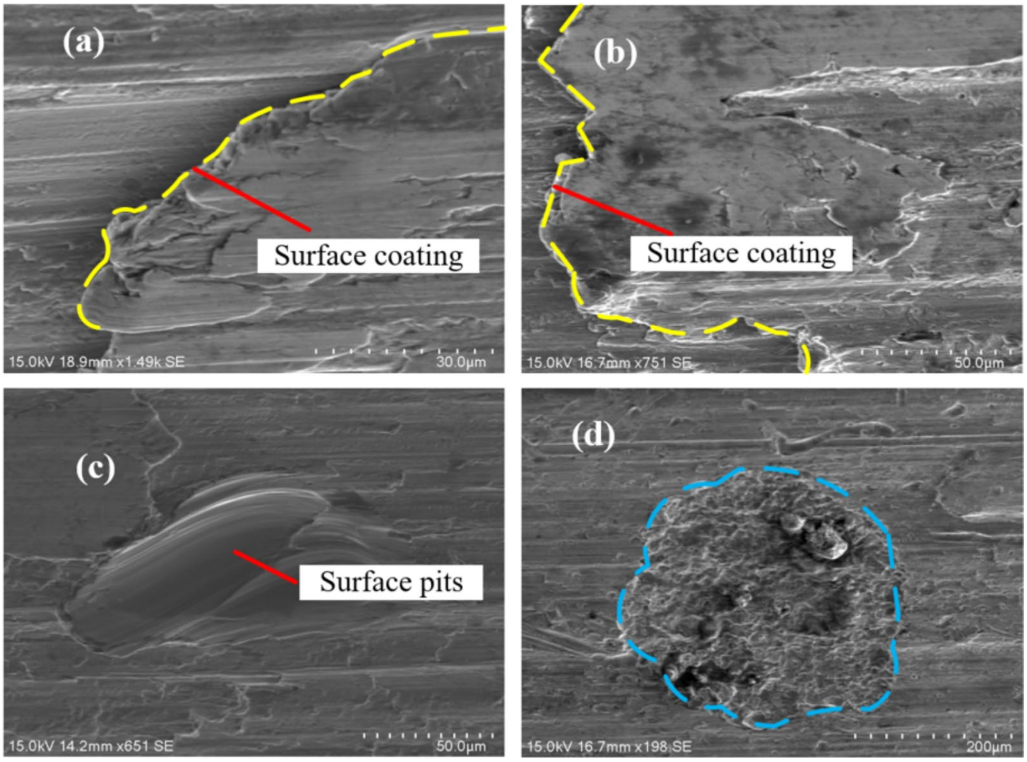

Figure 16 Surface coating and pits of contour bevel gear machined by dry milling

of the machined surface and deteriorates the surface quality.

EDS analysis of the machined surface of the contour bevel gear shows that location A in Figure 15(a) mainly contains three elements: Mn, Cr, and Fe, which are the same as the workpiece material, and it can be determined that it is the workpiece material. Location B in Figure 15(b) mainly contains three elements: O, Fe, and Mn, which are oxidized due to the adhesion of Fe elements. Therefore, it is inferred that location B is a mixture, which will reduce the hardness of the machined surface and toughness, thereby resulting in the deterioration of machined surface quality. The location C in Figure 15(c) contains mainly O, N, and Co elements, and it can be inferred that due to the oxidation reaction, it adheres to the machined surface and produces bumps, which affects the surface quality.

When milling contour bevel gears, due to the extrusion of the cutting edge, there are accumulation and coating on the machined surface. Figure 16(a) and (b) shows the micro morphologies of the convex and concave surfaces with v = 260 m/min, f = 0.3 mm/r. It can be seen from Figure 16(a) and (b) that, when coating occurs, the connection between the surface material and the substrate material is weak, and the surface material is easily peeled off, deteriorating the quality of the machined surface. In Figure 16(c) and (d), the surface morphologies at v = 170 m/min, f = 0.1 mm/r and v = 200 m/min, f = 0.1 mm/r, respectively, the surface quality of pits are poor due to the existence of partial workpiece material accumulation and coating on the machined surface resulting in local spalling of the workpiece surface and formation of surface pits. Therefore, surface defect behavior can be reduced by increasing the cutting speed and reducing the feed rate.

The surface defects are analyzed by EDS, as shown in Figure 17. It can be found that the energy spectrum of the defect is in good agreement with that of the matrix material, which confirms that the above defects are generated by the physical and mechanical effects of the workpiece and the tool in the cutting process, and no material outside the workpiece substrate is introduced.

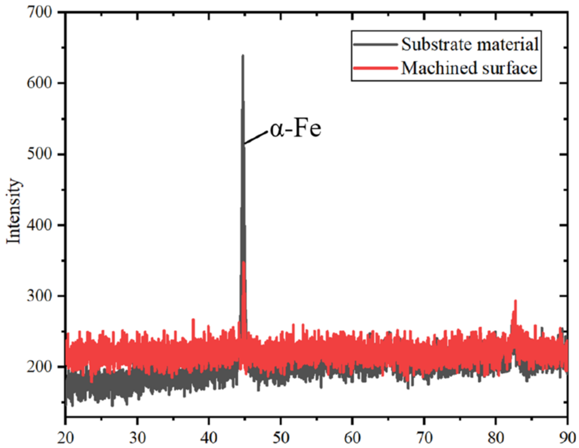

Figure 18 Comparative analysis of XRD diffraction results of machined surface and substrate

4.4 XRD Diffraction Analysis

XRD is used to compare and analyze the machined surface and substrate of 20CrMnTi. Figure 18 is a comparison of the diffraction spectrum of the machined surface and the substrate material. By comparing the XRD diffraction spectra of the substrate material and the machined surface, it can be found that the diffraction peak of the machined surface is higher than that of the substrate material. This is because the plastic deformation of the machined surface during the cutting process causes microscopic strains in the grains. Analysis of the diffraction peaks shows that the peak area is mainly α-Fe, which proves that there is a phase transition during

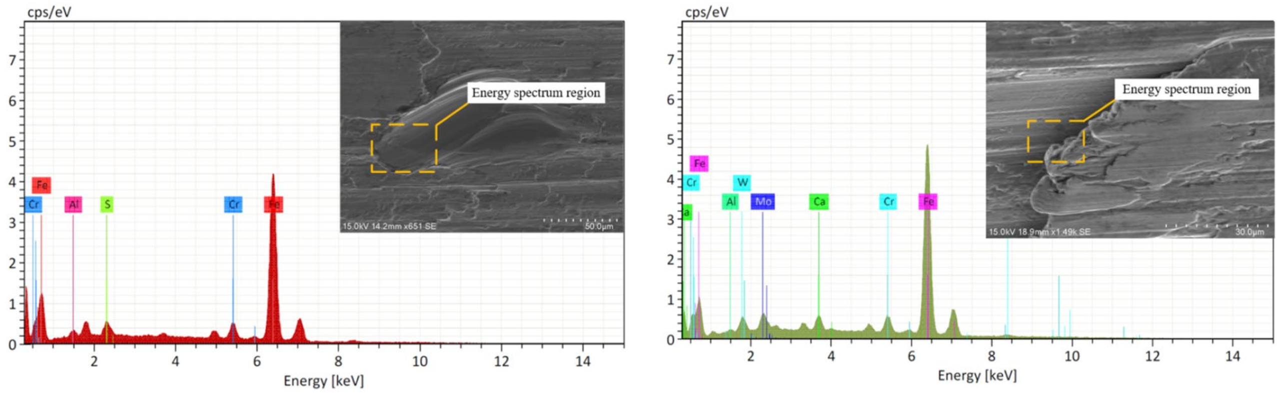

Figure 17 EDS analysis of surface pits and surface coating

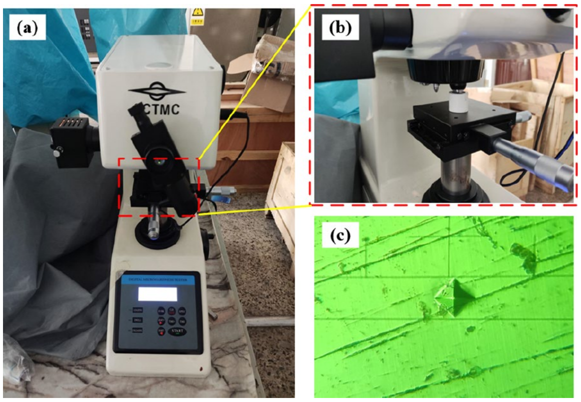

Figure 19 Microhardness measurement of machined surface

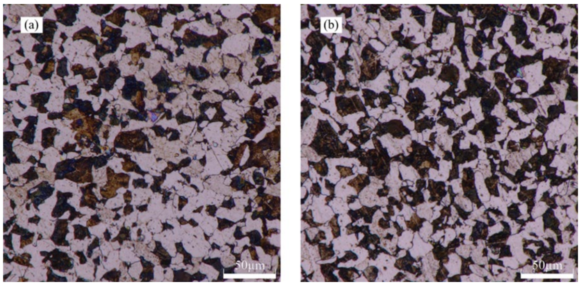

Figure 20 The metallographic microstructure of the machined surface (convex and concave)

processing and provides a basis for subsequent work hardening tests.

4.5 Analysis of Work Hardening on the Machined Surface of Contour Bevel Gears

DHV-1000 Vickers hardness tester is used to measure the hardness of the specimen. The load of the hardness experiment is 0.98 N, with a holding time of 15 s selected to ensure clear indentation, and the hardness value is calculated according to the geometric parameters. The measuring device is shown in Figure 19, and the hardness of the substrate material is measured at 165.9 HV.

It can be found from Table 6 that the hardness of the machined surface of the workpiece is greater than the hardness of the substrate. And the reason is that the metallographic microstructure of the substrate of the machined surface is ferrite, the black block distribution is lamellar pearlite, and the grains are fine. It can be inferred that due to the high temperature generated by the cutting process, the phase change of the substrate material occurs and lamellar pearlite is generated so that the strength and hardness of the machined surface are enhanced. Figure 20 shows the metallographic microstructures of the convex and concave surfaces of the machined surface.

Surface hardness measurements were performed on the concave and convex surfaces of the machined surfaces of the contour bevel gears, as shown in Tables 7 and 8. It can be found from Table 7 that the hardness value of the machined surface increases with the increase of cutting speed and then decreases, which is because with the increase of cutting speed, plastic deformation generated in the machined surface, and when cutting speed increases to 230 m/min, the cutting time is shortened and the cutting heat is not dissipated in time and leading to the enhancement of the thermal softening effect of the workpiece, so the degree of work hardening is reduced.

It can be found from Table 8 that the hardness of the machined surface increases as the feed increases, because the cutting force and plastic deformation zone increase with the increasing of feed rate, leading to the increases of work hardening, and the hardness values of the convex surface and the concave surface of the tooth surface are relatively close. Therefore, it is possible to appropriately increase the cutting speed and reduce the feed rate within a reasonable range, which is beneficial to reduce the work hardening behaviour of the machined surface.

Table 7 Microhardness variation of machined surfaces with cutting speed

Cutting speed (m/min)	**170**		**200**		**230**	
	Convex	**Convace**	**Convex**	**Convace**	**Convex**	**Convace**
Hardness value (HV)	179.3	180.2	184.7	183.5	177.3	176.8

Table 8 Microhardness variation of machined surfaces with feed rate

Feed rate (mm/r)	**0.1**		**0.2**		**0.3**	
	Convex	**Convace**	**Convex**	**Convace**	**Convex**	**Convace**
Hardness value (HV)	175.3	176.1	179.7	182.1	183.3	185.4

5 Conclusions

In this paper, in order to explore the machined surface quality of the contour bevel gear of dry milling, the single-factor test method is used to observe and analyze the machined surface morphology, surface defects and work hardening of the contour bevel gear; the influence of cutting speed and feed rate on machined surface quality is studied, and the main conclusions are as follows.

(1) The process of forming the machined surface roughness of contour bevel gears is analyzed through the principle of generation machining, which provides a basis for the experimental analysis of the machined surface quality of contour bevel gears.

(2) The analysis of the roughness and surface morphology of the machined surface shows that with the increase of cutting speed, the cutter pattern of the machined surface is gradually denser, and the residual height becomes smaller. The distance of the ridge lines on the morphology gradually increases, resulting in the deterioration of the machined surface quality. When the cutting speed is 230 m/min, the machined surface roughness is concentrated in the peak area, the roughness difference between the convex surface and the concave surface of the contour bevel gear is the smallest, and the formed surface quality is good. Using the machined surface roughness data of convex and concave surfaces, a surface roughness prediction model is established to provide guidance for optimizing the cutting parameters of contour bevel gears.

(3) The machined surface defects are analyzed by SEM, and the machined surface defects are found such as tool marks, surface adhesion, surface coating and surface pits. The energy spectrum analysis of the surface defect position show that the surface adhesion is partly due to the mixture of the adhering chips and the substrate material, and partly due to the oxidation reaction, resulting in oxide adsorption on the surface. The surface coating is due to the extrusion of the cutting edge, resulting in accumulation in the workpiece material and the formation of a surface pits after local spalling, Therefore, surface defects can be avoided by increasing the cutting speed and reducing the feed rate.

(4) Diffraction analysis of the substrate and machined surfaces by XRD reveal that the diffraction peak area is mainly α-Fe, which proves that there is a phase change during the machining process, which causes microscopic strain in the grains, resulting in an increase in the hardness of the machined surface. Machining hardening measurements on convex and concave surfaces of machined surfaces reveals that when the cutting speed is 230–260 m/min and the feed rate is 0.1mm/r, the degree of work hardening of the machined surface is low. Therefore, machining of contour bevel gears within this range will reduce the work hardening behavior of the workpiece.

Acknowledgements
Not applicable.

Author Contributions
MW conceived the idea of the study; JZ was in charge of the whole trial and revised the manuscript; CM, YZ assisted in completing the experiment and data collection; YC contributed to refining the ideas and finalizing this manuscript; all authors read and approved the final manuscript.

Authors' Information
Mingyang Wu, born in 1971, is currently a professor at *School of Mechanical Power Engineering, Harbin University of Science and Technology, China.* He received his PhD degree from *Harbin Engineering University, China*, in 2008. His research focuses on efficient machining technology for difficult-to-cut materials and tool technology. E-mail: 13936161878@139.com
Jianyu Zhang, born in 1996, is currently a master candidate at *School of Mechanical Power Engineering, Harbin University of Science and Technology, China.* His research focuses on high-speed cutting technology, metal cutting principles and tools. E-mail: a838232529@163.com
Chunjie Ma, born in 1996, is currently a master candidate at *School of Mechanical Power Engineering, Harbin University of Science and Technology, China.* His research focuses on high-speed cutting technology, metal cutting principles and tools. E-mail: mcj199638@163.com
Yali Zhang, born in 1996, is currently a master candidate at *Mechanical Power Engineering, Harbin University of Science and Technology, China.* His research focuses on high-speed cutting technology, metal cutting principles and tools. E-mail: yali18846130501@163.com
Yaonan Cheng, born in 1977, is currently a professor at *School of Mechanical Power Engineering, Harbin University of Science and Technology, China.* He received his PhD degree from *Harbin University of Science and Technology, China*, in 2008. His research focuses on heavy cutting theory and tool technology, groove optimization technology and efficient machining technology for difficult-to-machine materials. E-mail: yaonancheng@163.com

Funding
Supported by National Key R&D Program of China(Grant No. 2019YFE0121300) and Yancheng Hali Power Transmission and Intelligent Equipment Industrial Research Institute Project.

Availability of data and materials
The datasets supporting the conclusions of this article are included within the article.

Competing Interests
The authors declare no competing financial interests.

Received: 28 November 2021 Revised: 15 August 2022 Accepted: 28 November 2022

References

[1] J Han, G Zhang. Investigation on formation mechanism of surface texture and modeling of surface roughness with internal gear power honing. *The International Journal of Advanced Manufacturing Technology*, 2018, 98(1-4): 603-615.

[2] S Khalilpourazary, S Meshkat. Investigation of the effects of alumina nanoparticles on spur gear surface roughness and hob tool wear in hobbing process. *The International Journal of Advanced Manufacturing Technology*, 2014, 71(9-12): 1599-1610.

[3] X Ming, Q Gao, H Yan, et al. Mathematical modeling and machining parameter optimization for the surface roughness of face gear grinding. *The International Journal of Advanced Manufacturing Technology*, 2017, 90(9-12): 2453-2460.

[4] S Pathak, N K Jain, I A Palani. Effect of honing gear hardness on microgeometry and surface quality improvement of straight bevel gears in PECH process. *The International Journal of Advanced Manufacturing Technology*, 2016, 85(9-12): 2197-2205.

[5] J Michalski. Surface topography of the cylindrical gear tooth flanks after machining. *The International Journal of Advanced Manufacturing Technology*, 2009, 43(5-6): 513-528.

[6] F Klocke, C Gorgels, A Stuckenberg. Investigations on Surface Defects in Gear Hobbing. *Procedia Engineering*, 2011, 19: 196-202.

[7] J Han, B Yuan, D Wang, et al. Formation mechanism study on tooth surface of two gear finishing processes: combined theoretical and experimental approaches. *Journal of the Brazilian Society of Mechanical Sciences and Engineering*, 2017, 39(12): 5159-5170.

[8] F Zheng, M Zhang, W Zhang, et al. The fundamental roughness model for face-milling spiral bevel gears considering run-outs. *International Journal of Mechanical Sciences*, 2019, 156: 272-282.

[9] V Simon. Improvements in the micro tooth surface topography of hobbed spur and helical gears. *Journal of the Brazilian Society of Mechanical Sciences and Engineering*, 2018, 40(4): 1-8.

[10] H Hassanpour, M Sadeghi, A Rasti, et al. Investigation of surface roughness, microhardness and white layer thickness in hard milling of AISI 4340 using minimum quantity lubrication. *Journal of Cleaner Production*, 2016, 120: 124-134.

[11] S Mao, X Wu, G Nie. The equal TSR grinding method on gear grinding machines with conical wheels. *Tool Engineering*, 1998, 10(6): 13–15.

[12] J Lin, C Teng, X Li, et al. Tooth profile deviation measurement of cylindrical gears based on a roughness profilometer. *Chinese Journal of Scientific Instrument*, 2020, 41(12): 15-22.

[13] S Bin, Z Cai. Modeling and analysis of surface roughness for generating grinding of face gear. *Journal of Wuhan University (Engineering Edition)*, 2021, 54(6): 571-578.

[14] J Ma, Z Gou, P Zhu, et al. Reaearch on surface roughness of skived gear quenched. *Optics and Precision Engineering*, 1995(4): 82-86.

[15] N Gao. Research on surface roughness of 20CrMnTi gear hobbing. *Machine Design and Manufacturing Engineering*, 2021, 50(7): 122-124.

[16] T Li, X Deng, J Li, et al. Automatic feedback correction and deviation analysis for tooth surface of spiral bevel and hypoid gear. *Journal of Aerospace Power*, 2011, 26(5): 1194-1200.

[17] Z Wang, T Zeng. Correction of tooth flank errors of spiral bevel gear based on proportional change parameters. *Journal of Mechanical Engineering*, 2010, 46(1): 43-47.

[18] X Wen, Y Zhao. The study of three dimensional surface roughness. *Metrology & Measurement Technique*, 2001(6): 13-14.